Capacitor-based Activity Sensing for Kinetic-powered Wearable IoTs

GUOHAO LAN, Duke University, USA
DONG MA, University of New South Wales, Australia
WEITAO XU, City University of Hong Kong, China
MAHBUB HASSAN and WEN HU, University of New South Wales, Australia

We propose the use of the conventional energy storage component, i.e., capacitor, in the kinetic-powered wearable IoTs as the sensor to detect human activities. Since activities accumulate energy in the capacitor at different rates, the charging rate of the capacitor can be used to detect the activities. The key advantage of the proposed capacitor-based activity sensing mechanism, called CapSense, is that it obviates the need for sampling the motion signal at a high rate, and thus, significantly reduces power consumption of the wearable device. The challenge we face is that capacitors are inherently non-linear energy accumulators, which leads to significant variations in the charging rates. We solve this problem by jointly configuring the parameters of the capacitor and the associated energy harvesting circuits, which allows us to operate in the charging cycles that are approximately linear. We design and implement a kinetic-powered shoe and conduct experiments with 10 subjects. Our results show that CapSense can classify five different daily activities with 95% accuracy while consuming 57% less system power compared to conventional motion-sensor-based approaches.

CCS Concepts: • **Computing methodologies** → **Activity recognition and understanding**; • **Human-centered computing** → **Ubiquitous computing**;

Additional Key Words and Phrases: Kinetic energy harvesting, capacitor, activity recognition, wearable IoTs

ACM Reference format:
Guohao Lan, Dong Ma, Weitao Xu, Mahbub Hassan, and Wen Hu. 2020. Capacitor-based Activity Sensing for Kinetic-powered Wearable IoTs. *ACM Trans. Internet Things* 1, 1, Article 2 (February 2020), 26 pages.
https://doi.org/10.1145/3362124

1 INTRODUCTION

The rapid development of wearable IoTs [46] has enabled many human-centric monitoring services, such as step-counting [9], elder fall-detection [38], and daily activity recognition [19]. Conventionally, activity monitoring is achieved by sampling a time-series of the motion signal, e.g., the 3-axial accelerations, 25–100 times per second [7, 30], depending on the performance

Most of the work was done while the author was with the University of New South Wales, Sydney, Australia.
Authors' addresses: G. Lan, Duke University, Department of Electrical and Computer Engineering, 100 Science Dr, Durham, NC, 27708, United States; email: guohao.lan@duke.edu; D. Ma (corresponding author), M. Hassan, and W. Hu, University of New South Wales, School of Computer Science and Engineering, Building K17, Kensington Campus, Sydney, NSW, 2052, Australia; emails: dong.ma1@student.unsw.edu.au, {mahbub.hassan, wen.hu}@unsw.edu.au; W. Xu, City University of Hong Kong, Department of Computer Science, 83 Tat Chee Avenue, Kowloon Tong, Hong Kong; email: weitaoxu@cityu.edu.hk.

2577-6207/2020/02-ART2 $15.00
https://doi.org/10.1145/3362124

requirements (i.e., accuracy and latency). Although wearable devices can provide a variety of monitoring and tracking services, the high power consumption due to the continuous sampling of the motion signal limits their pervasive use.

In general, the power consumption in sampling is directly proportional to the sampling rate, as the higher the sampling rate, the more power is consumed by the sensors as well as the microcontroller (MCU), which has to wake up more frequently to read, process, and store the samples. A large volume of past research on mobile sensing, therefore, has focused on reducing the sampling rates of accelerometer-based systems [42, 54]. More recently, researchers have investigated the use of kinetic energy harvesting (KEH) transducer as the sensor to detect different contexts [5, 13, 17, 20, 25, 52]. The instantaneous electric voltage signal generated by the energy harvesting transducer is used as an alternative to the acceleration signal. Transducer-based sensing method introduces new power-saving opportunities for power-limited wearable devices as, unlike the accelerometers, transducers themselves do not consume any external power. Thus, by saving the energy that would have otherwise been consumed by the accelerometer, transducer-based systems can further reduce the sampling power consumption [20]. However, as transducer-based approach relies on a time-series of signal as the input for activity recognition, it still requires the MCU to frequently wake up, and thus, consumes a considerable amount of power in energy-limited wearable devices.

In this article, we propose a new way to detect activities for kinetic-powered wearable IoTs, which obviates the need for frequent motion signal sampling and allows very aggressive duty cycling of the MCU to reduce power consumption by several orders. To achieve this goal, the proposed system, which we call CapSense, capitalizes on two important observations:

(1) **The kinetic power of human activities is distinct.** It has been widely demonstrated in the literature that the kinetic energy harvested from different activities is distinctively different [12, 56]. Thus, the energy generation rate of the kinetic-powered wearable device can be used as a feature for human activity recognition.
(2) **Capacitor provides accumulated information**. In kinetic-powered devices, the energy generated by the energy harvesters is naturally stored in the associated capacitor. Moreover, the charging rate of the capacitor provides information about the *energy generation rate* of the external activity. In addition, charging rate of the capacitor can be obtained by simply reading the capacitor voltage at the end of each detection period, which is typically about five seconds [7, 31], without the need of sampling the instantaneous signal many times during this period.

Thus, it should be possible to classify human activities by simply reading the capacitor voltage only once every few seconds. Comparing with conventional motion-sensor-based activity detection, which requires the system to wake up many times per second [30], CapSense allows very aggressive duty cycling of the embedded IoT.

However, in realizing CapSense, we face two challenges. The first challenge comes from the fundamental charging property of the capacitor [50], as the capacitor becomes harder charge with more energy accumulated. Thus, even for the same activity that generates the same amount of energy, the charging rate of the capacitor decreases with the increase of its voltage level. The second challenge arises due to use of a *simple* and *single* feature, i.e., the capacitor charging rate, for activity sensing. In contrast, conventional motion-sensor-based methods leverage a time-series of motion signal and a set of features for recognition. Both challenges must be addressed to realize acceptable activity classification accuracy for CapSense. The contributions of this article can be summarized as follows:

(1) We propose a new method for human activity sensing, CapSense, which detects activity from the charging rate of the energy storing capacitor.

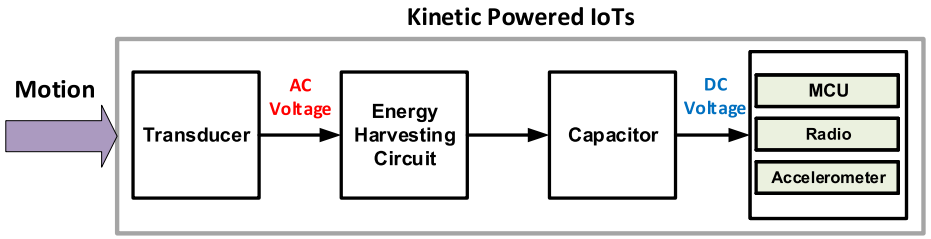

Fig. 1. Generic architecture for kinetic-powered IoT device. The kinetic energy is converted by the transducer and will be stored in the capacitor before it is sufficient to power the user loads.

(2) We address the challenge of non-linear capacitor charging by jointly configuring the parameters of the capacitor and the associated energy harvesting circuits. Our solution ensures approximately linear capacitor charging cycles during the sensing operation.
(3) We implement CapSense using the piezoelectric bending energy harvester in the form factor of shoe. We address the single feature classification challenge by introducing two energy harvesters and capacitors—one at the rear of the sole and the other at the front. Using our dual-capacitor prototype, we conduct experiments with 10 subjects performing five different activities. We demonstrate that CapSense is capable of detecting daily activity with up to 95% accuracy.
(4) We conduct a detailed power profiling to quantify the power-saving opportunity of CapSense. Our measurement results indicate that, compared to the state-of-the-art, CapSense reduces sampling-related power consumption by 54% and the overall system power consumption by 57%.

Partial and preliminary results of this article have appeared in our previous work [27]. In this article, we provide the following two major extensions to the conference version: (1) we redesign the CapSense prototype by adding a second energy harvester and capacitor to the shoe insole (at the front), and thus realize the *dual-capacitor* wearable prototype; and (2) we conduct a new set of experiments and collect a new dataset for the dual-capacitor prototype. Using the new dataset, we demonstrate that the new design improves the activity recognition accuracy by 11% compared to a single capacitor system.

The rest of the article is organized as follows: We first introduce the background of kinetic-powered IoTs in Section 2. Then, we present the design and implementation of CapSense in Section 3, followed by its performance evaluation in Section 4. The power measurement study is presented in Section 5. We review the related works in Section 6 before we conclude the work in Section 7.

2 PRELIMINARIES IN KINETIC-POWERED IOT

In this section, we provide the basic background of kinetic-powered IoTs and the concept of kinetic energy harvesting transducer-based sensing.

2.1 Kinetic Energy Harvesting

Kinetic energy is the energy of an object's motion. Kinetic Energy Harvesting (KEH) refers to the process of scavenging the kinetic energy that is released from the human activity or the ambient vibrations. The use of KEH for self-powered IoTs has been widely investigated in the literature [4, 37]. Figure 1 shows a generic architecture of a kinetic-powered IoT device, which typically contains a transducer, i.e., energy generator, that converts the mechanical energy into electric AC voltage,

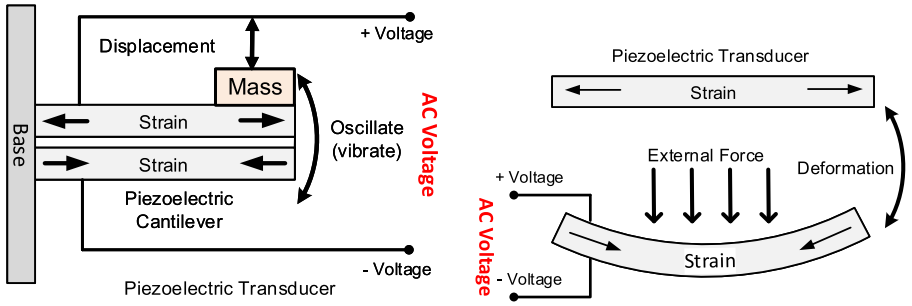

(a) Inertial-force transducer (b) Direct-force transducer.

Fig. 2. Principle of kinetic energy harvesting transducer.

a set of energy harvesting circuits that converts the AC voltage into regulated DC output, and the energy storage element, e.g., a capacitor, that stores the harvested energy. The stored energy will be used to power external user loads (e.g., sensors, MCU, or radio) when a sufficient amount of energy has been accumulated.

There are three main energy transduction techniques that are widely used in the literature: *piezoelectric*, *electromagnetic*, and *electrostatic*. Among them, piezoelectric is the most favorable transduction mechanism for wearable IoTs, because of its simplicity and compatibility with MEMS (micro electrical mechanical system). Fundamentally, the three techniques share the same physical mechanism to convert the kinetic energy into electric power. Depending on the energy harvesting scenario, transducers can be classified into two different categories: the inertial-force transducer and the direct-force transducer [37]. As shown in Figure 2(a), the inertial-force transducer is usually modeled as an inertial oscillating system consisting of a cantilever beam attached with two piezoelectric outer-layers. One end of the cantilever is fixed to the device, while the other end is set free to oscillate (vibrate). When the piezoelectric cantilever is subjected to a mechanical stress, it expands on one side and contracts on the other. The induced piezoelectric effect will generate an AC voltage output as the beam oscillates around its neutral position. Similarly, in terms of the direct-force transducer shown in Figure 2(b), the AC voltage signal is generated when the piezoelectric transducer is deformed (bent) by the external mechanical force. In this article, we build our proof-of-concept prototype using the direct-force piezoelectric transducer (in Section 3.3).

2.2 KEH-transducer-based Sensing

Although KEH transducer is designed with the purpose of scavenging kinetic energy from motions, researchers have investigated the use of KEH-transducer as a low-power vibration sensor for context detection [17, 20, 32], in which the AC voltage generated by the transducer is used as the signal for sensing. Comparing with conventional vibration sensor, e.g., accelerometer, KEH-transducer-based system is able to eliminate the energy consumed by the motion sensor. For instance, in Reference [20], a KEH-transducer-based activity recognition system is designed, and it is able to achieve 83% of accuracy for classifying different daily activities while saving 79% of the power that will be consumed by an accelerometer. Similarly, in Reference [32] the AC voltage signal harvested from the airflow is used to monitor the usage of the air-conditioning system. Recently, the voltage signal generated from human gaits is applied for mobile user authentication [52].

3 SYSTEM OVERVIEW

In this section, we present the concept, design, and implementation of CapSense.

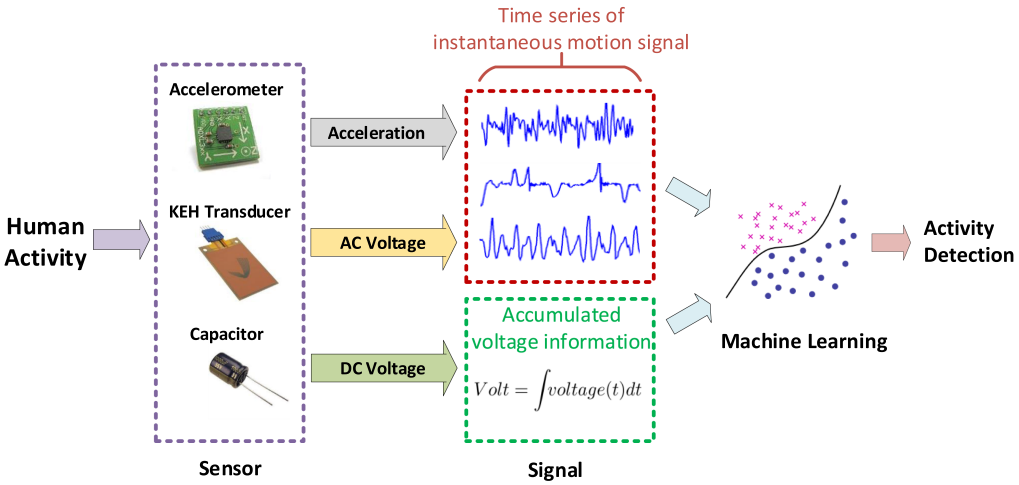

Fig. 3. The processing pipeline of a typical activity sensing system. Comparing with both accelerometer and KEH-transducer-based system, CapSense does not require any time-series of motion signal for classification.

3.1 CapSense Concept

Figure 3 shows the processing pipeline of a typical activity sensing system. It has a sequence of procedures, including data sampling, signal processing, feature extraction, and utilizes machine learning algorithms for classification. We can notice that for both accelerometer and KEH-transducer-based sensing systems, ***a time-series of instantaneous motion signal*** (either acceleration or AC voltage signal) is required as the input for activity detection. This time-series of signal is usually obtained by sampling the motion sensor at a frequency of 25–100 Hz given different accuracy requirements [7]. This implies that the MCU of the IoT device must wake up at least 25–100 times per second to acquire the instantaneous motion signal. As we will demonstrate later in Section 5, a large fraction of the sampling power is actually consumed by the MCU. Although the use of KEH-transducer can eliminate the energy consumption in powering the sensors, it still needs to continuously sense and process the AC voltage signal from the KEH-transducer at a high sampling rate. Thus, it will consume a significant amount of the harvested energy. This motivates the design of CapSense, which aims to achieve high recognition accuracy while eliminating the need of high-frequency data sampling.

As shown in Figure 3, unlike accelerometer or KEH-transducer-based systems that sample *a time-series of instantaneous motion signal* from the sensor, CapSense uses *a single sample* of the capacitor voltage for activity recognition. The feasibility of CapSense relies on two fundamental facts:

Fact 1. **The kinetic power of diferent human activities are distinct**. It has been widely demonstrated in the literature that the kinetic power harvested from different activities is different [12, 56]. Thus, the energy generation rate of the kinetic-powered wearable device can be used as a feature for human activity recognition.

Fact 2. **Capacitor provides accumulated information**. As shown in Figure 1, in the kinetic-powered devices, the energy generated by KEH-transducer is stored in the associated capacitor. Thus, the capacitor charging rate provides information about the *energy generation rate* of the external activity. As it will be shown in Section 3.5, the capacitor's charging rate over the last T_C second(s) can be estimated by simply reading

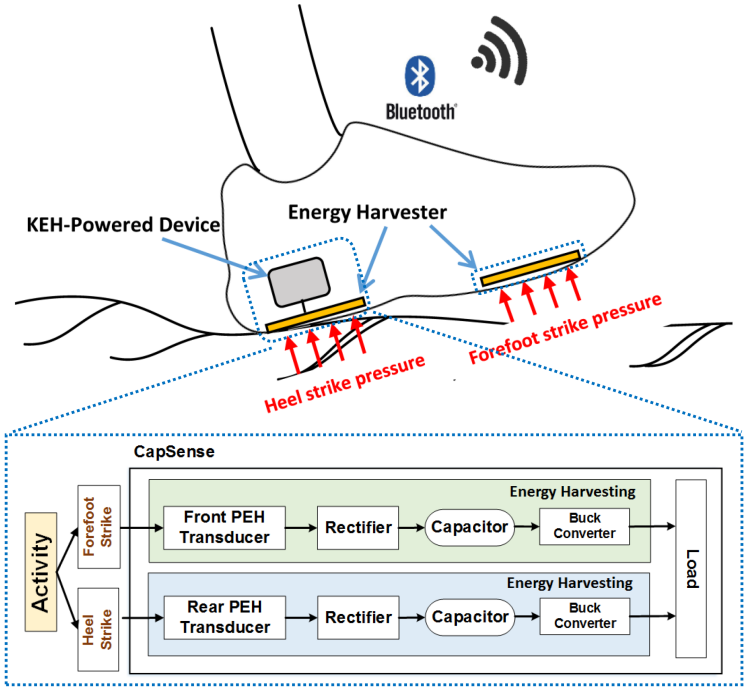

Fig. 4. System architecture of CapSense.

the capacitor voltage once every T_C second(s), without the need of sampling the AC voltage signal frequently to calculate the average harvesting power.

Those two facts imply that by using the charge of the capacitor voltage over a time period of T_C, we can estimate the corresponding energy generation rate and use it to recognize the activity in the last T_C period of time. As we will demonstrate later in Section 4, CapSense can detect activities by reading the capacitor voltage once every $T_C = 5$ seconds compared to tens of Hz required by the state-of-the-art [7, 20]. The fundamental novelty of CapSense is that, unlike accelerometer or KEH-transducer that can only provide instantaneous motion information of the subject at a particular time, capacitor accumulates the generated KEH energy over time, and the capacitor voltage provides the ***accumulated information*** of the subject over a period of time. Thus, it allows very aggressive duty cycling of the MCU and reduces the sensing-induced power consumption by several orders. Below, we introduce the design and implementation of CapSense.

3.2 CapSense Architecture

There is a variety of options in the design of KEH-powered wearable devices, such as backpack [51], fabric [55], wristband [45], and footwear [24, 48]. We designed our system in the form-factor of shoes for several reasons: first, shoes are worn by the users for the majority of time in their daily lives; second, unlike many other wearable devices, shoes have a much larger space to place the energy harvesters; third, it is known that feet can generate more energy than the other body parts [3, 15].

Figure 4 shows the system architecture of CapSense. Considering the scenario in which a subject is wearing the KEH-powered shoes and doing some activities, e.g., walking or running, her foot will hit the ground floor and the pressure induced by both the heel and the forefoot strikes will

bend the two piezoelectric energy harvesters (PEH) placed inside the shoe. The PEH will generate electric power from the foot strikes when the subject is doing different activities. The generated energy is accumulated in the associated capacitor. As discussed, since the power generated from different human activities is distinctively different [12], and the energy generated by the PEH within the last T_C second(s) is accumulated in the capacitor, it would be possible to estimate the power generation rate during T_C by a single reading of the capacitor voltage. Then, the estimated rates can be used to recognize the activity that was performed by the user in the last T_C second.

As shown in Figure 4, CapSense consists of two parts: *Load* and *Energy Harvesting*. The *Load* represents the system components that are responsible for data sensing, processing, and communication (or it can be a rechargeable battery that is used to power a wearable system). The *Energy Harvesting* corresponds to the functional components that harvest and accumulate energy from the human activity. It includes two PEH transducers, i.e., the front and the rear PEH transducers, to harvest energy from the foot strikes. As exhibited in Figure 4, the front PEH transducer is able to harvest energy from the ground reaction pressure associated with the toe-off phases when the forefoot hits the ground, while the rear PEH transducer is designed for harvesting energy from the pressure caused by the heel strikes. More specifically, when the subject is walking/running, the body-weight-induced pressure will be transferred to the PEH transducers through bones [22]. Given the anatomical structure of the foot, the front PEH is placed at the location to capture the pressure transferred from the metatarsal bones, while the rear PEH is placed at the location to capture the pressure from the calcaneus (heel) bone. In CapSense, the two PEH transducers are connected to the rectifying circuits that rectify the intermittent AC voltage into stable DC power. The rectified DC voltage is accumulated in the corresponding capacitor before it is sufficient to turn on the *buck converter* (i.e., the voltage of the capacitor should reach a pre-defined threshold that is configured in the buck converter).

3.3 CapSense Prototype Design

Figure 5(a) shows the design and the implementation of CapSense. As discussed, the prototype consists of two parts: the *Energy Harvesting* and the *Load*. For the Energy Harvesting part, we select two EH220-A4-503YB PEH bending transducers from the Piezo Systems[1] as our PEH transducers and attach them to the shoe-pad. The transducers are 10.4 grams each with a dimension of $76.2 \times 31.75 \times 2.28\ mm^3$, which makes them easy to place inside the shoe. As shown in Figure 5(a), the two PEH transducers are fixed at the front and the rear of the shoe-pad to harvest energy from the heel and forefoot strikes, respectively. The details of the PEH transducers are given in Figure 5(b).

The output pins of the PEH transducer are connected to an energy harvesting circuit, namely the LTC3588-1 from the Linear Technology.[2] The LTC3588-1 integrates a low power-loss bridge rectifier that can rectify the AC voltage output from the PEH transducer, and a high-efficiency buck converter that can transfer the energy stored in the capacitor into stable DC power to charge the load. We select two electrolytic capacitors with capacitance of 470 μF and rating voltage (i.e., the maximum voltage) of 25 V to store the generated energy from the two PEH transducers (we will discuss how we select the capacitor in Section 3.4). When the voltage of the capacitor rises above the undervoltage lockout rising threshold of the buck converter (i.e., denoted by $V_{UVLO}\ rising$, and equals to $4V$ in our setting), the buck converter will be enabled to discharge the energy that is stored in the capacitor. However, when the capacitor voltage is discharged below the lockout falling threshold (i.e., denoted by $V_{UVLO}\ falling$, and equals to 3.08 V in our setting), the buck

[1]Piezo System: http://www.piezo.com/prodexg8dqm.html.
[2]LTC3588: http://www.linear.com/product/LTC3588-1.

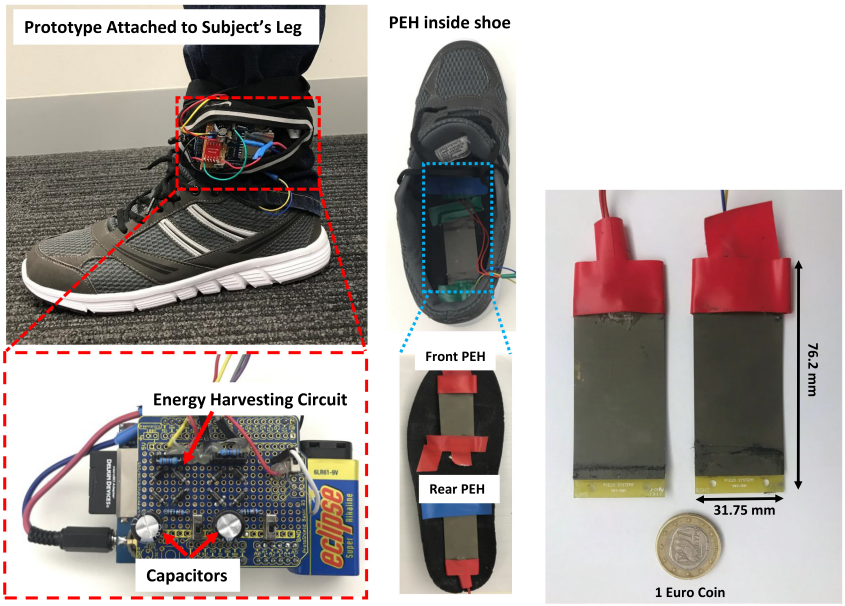

(a) CapSense prototype. (b) PEH Transducers.

Fig. 5. CapSense prototype design.

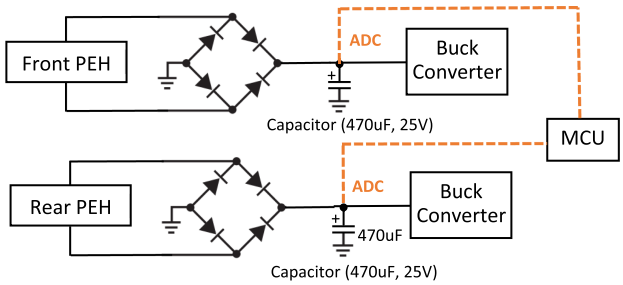

Fig. 6. CapSense overall circuit design.

converter will be turned off, and the capacitor starts to accumulate the energy generated by the PEH transducer.

The simplified circuit diagram of the prototype is shown in Figure 6. The front and the rear capacitors are used to store the energy harvested from the two PEHs. For analysis purposes, the voltage of the two capacitors and the AC voltage generated by the two PEHs are sampled through the onboard 10-bit ADC of an Arduino Uno board. The sampling rate is fixed at 100 Hz. The sample data are stored on the SD card for offline data analysis. By using this data, we will analyze the performance of CapSense and demonstrate that it is able to achieve over 90% classification accuracy by sampling the capacitor voltage once every five seconds.

3.4 Ensuring Linearity in Capacitor Voltage

Before presenting the details of capacitor-based sensing, we first analyze some properties of the capacitor when it is powered by an energy harvester. We also discuss the feasibility and design requirement in leveraging the capacitor voltage for activity sensing.

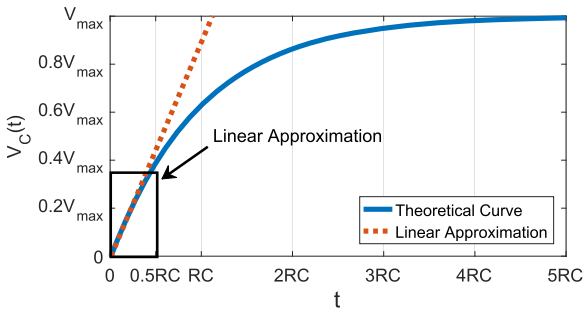

Fig. 7. The theoretical curve shows the voltage of the capacitor $V_C(t)$ when it is charged over time t. The theoretical curve is approximated by a linear curve. The unit of t is RC (i.e., the time constant).

The voltage of the capacitor, $V_C(t)$, at time t during the charging is given by:

$$V_C(t) = V_{max}\left(1 - e^{-t/\tau}\right), \tag{1}$$

where V_{max} is the maximum voltage to which the capacitor can be charged, and it is bounded by $V_{max} = min\{V_{rating}, V_S\}$, in which V_S is the supply voltage applied to the capacitor, and V_{rating} is the rating voltage of the capacitor; constant τ is defined as $\tau = RC$, in which R is the resistance of the resistor in the equivalent resistor-capacitor charging circuit (RC circuit), and C is the capacitance of the capacitor. For a given capacitor, τ is known as the *time constant* of the equivalent RC circuit, which is a constant value (in seconds).

The relation between the capacitor voltage, $V_C(t)$ and time t is visualized in Figure 7. The theoretical curve indicates the voltage of the capacitor when it is charged by the supply voltage V_S over time (in our case, V_S is the rectified DC voltage from the rectifier). We can observe that, within the examining time of $5RC$, $V_C(t)$ increases exponentially and its increasing rate is not constant. For instance, $\Delta V_C(t)$ in the first RC interval (i.e., from time 0 to RC) is not equal to that in the second RC interval (i.e., from time RC to $2RC$). As we will discuss later in Section 3.5, the only information we can obtain from the capacitor is its voltage, and we will use the voltage increasing rate for activity sensing. Thus, the nonlinear increment in the capacitor voltage will introduce additional variation and impair the activity recognition accuracy. In other words, due to the nonlinear charging behavior of the capacitor, the voltage increasing rate of the capacitor changes over time even if the capacitor is charged by a constant suppy voltage V_S.

Fortunately, as we can see in Figure 7, with time $t \leq \frac{1}{2}RC$, the theoretical curve of V_C (defined in Equation (1)) can be approximated by a linear curve [35]. According to the RC circuit theory, a capacitor can be charged to 39.3% of V_{max} with a charging time of $\frac{1}{2}RC$. It means that to ensure the linearity in the capacitor voltage for a maximum time of $\frac{1}{2}RC$, V_{max} should satisfy:

$$V_{max} \geq \frac{V_{UVLO\ rising}}{0.393}, \tag{2}$$

which yields:

$$min\{V_{rating}, V_S\} \geq \frac{V_{UVLO\ rising}}{0.393}, \tag{3}$$

where $V_{UVLO\ rising}$ is the undervoltage lockout rising threshold of the buck converter, at which the capacitor starts to be discharged. This means that, to ensure the linearity in the capacitor voltage, the selection and configuration of the hardware components (i.e., the PEH transducer, the buck converter, and the capacitor) should be considered interactively.

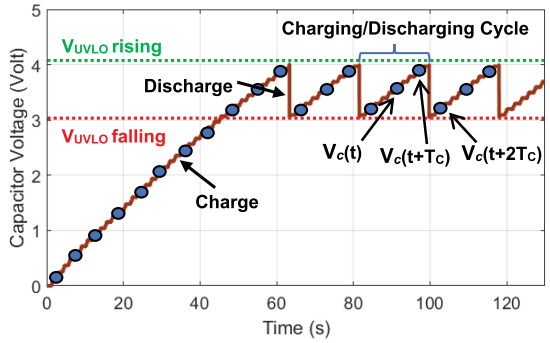

Fig. 8. Voltage trace showing the capacitor is charged and discharged periodically. The blue dots indicate the possible sampling points at which the MCU wakes up to read the capacitor voltage.

As discussed in Section 3.3, in our prototype, the V_{UVLO} *rising* of the buck converter is configured as 4 V.[3] Thus, given Equation (3), we have: $min\{V_{rating}, V_S\} \geq \frac{4V}{0.393} = 10.18V$. The value of the rectified DC voltage, V_S, is depending on the energy harvester that is used in the system. Given different materials and configurations of the energy harvester, V_S can be as high as tens of volts. In our case, the rectified voltage generated by the PEH transducer is up to 20.8 V, which is much higher than 10.18 V. Therefore, the rating voltage of the capacitor, V_{rating}, should be larger than 10.18 V. In our design, we select our capacitor with the rating voltage of 25 V to meet the requirement.

3.5 Activity Sensing Using Capacitor Voltage

In the following, we discuss how to use the capacitor voltage for activity sensing. Figure 8 shows the charging and discharging cycles of the capacitor when it is powered by the energy harvester. The charging/discharging behavior of the capacitor is controlled by the energy harvesting circuit. Initially, the capacitor voltage starts from 0 and takes approximately 60 seconds to reach 4 V. Then, it triggers the buck converter to discharge the accumulated energy (i.e., the V_{UVLO} of the buck converter is 4 V). When the capacitor voltage is discharged to 3.08 V, the buck converter shuts off until the capacitor voltage reaches the V_{UVLO} rising threshold again.

During the charging/discharging of capacitor, CapSense duty-cycles the MCU to periodically sample the capacitor voltage. An example is shown in Figure 8. The MCU wakes up to sample the capacitor voltage once every T_C seconds. By using any two adjacent voltage samples, we can estimate the capacitor voltage increment rate, r, over the last accumulation time of T_C:

$$r = \frac{V_C\,(t + T_C) - V_C\,(t)}{T_C},\ s.t.\ V_C\,(t + T_C) > V_C\,(t), \tag{4}$$

where $V_C\,(t)$ and $V_C(t + T_C)$ are the capacitor voltage at time t and $t + T_C$, respectively. That is to say, by periodically sampling the capacitor voltage at a frequency of $\frac{1}{T_C}$Hz, we can estimate the energy generation rate of the PEH transducer (either the front or the rear PEH transducer in our prototype) over the last T_C seconds. Note that MCU has no knowledge about the charging/discharge status of the capacitor; it is possible that the two adjacent voltage samples are obtained in different charging cycles. For instance, as shown in Figure 8, it may result in the case where $V_C\,(t + T_C) \geq V_C\,(t + 2T_C)$. Consequently, it will lead to a negative r in the estimation. This is because the capacitor is discharged after time $t + T_C$ while the capacitor voltage $V_C\,(t + 2T_C)$

[3] According to the datasheet of LTC3588, to ensure an output DC voltage of 2.5 V, the lowest voltage threshold is 4 V.

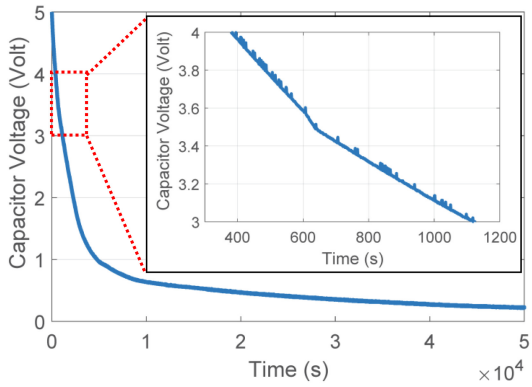

Fig. 9. The measured voltage of a self-discharge capacitor.

is sampled at the initial charging state in a new charging cycle. To avoid this, when estimating the voltage increment rate, we disregard all adjacent voltage peers $\{V_C(t), V_C(t+T_C)\}$ in which $V_C(t+T_C) \leq V_C(t)$.

3.5.1 Impact from the Capacitor Discharging. The estimation of r may be affected by the discharging time of the capacitor. As if it takes a long time for the buck converter to discharge the capacitor from 4 V to 3 V, it is possible that the MCU wakes up and reads an incorrect voltage value when the capacitor is still discharging, which means the capacitor discharge happens in the middle of the last T_C seconds, such that the actual energy accumulation time is shorter than T_C. Consequently, the voltage increment rate r obtained from Equation (4) will be underestimated. Fortunately, as shown in Figure 8, the time required by the buck converter to discharge the capacitor from 4 V to 3 V is less than 10 *ms*, according to our measurement. This fast discharging speed ensures that whenever a capacitor discharge happens within the last T_C seconds, the measured voltage $V_C(t+T_C)$ will be much lower than $V_C(t)$, and thus will be disregarded during the estimation.

3.5.2 Impact from the Capacitor Self-discharge. Another factor that may affect the estimation of r is the self-discharge of the capacitor; that is, the voltage leakage of the capacitor when it is not charged by the energy harvester. A high voltage leakage may result in an underestimation in r, as part of the harvested energy is discharged. To investigate the impact of capacitor leakage, we measured the voltage of our capacitor when it self-discharges from 5 V to 0 V. The results are shown in Figure 9. Specifically, we are interested in the behavior of the capacitor within the 3–4 V range. As shown in the amplified subfigure, we can see that it takes more than 700 seconds (i.e., 12 minutes) for the capacitor to self-discharge from 4 V to 3 V, which means that the leakage of the capacitor is negligible within a few seconds. Thus, the capacitor leakage has a negligible impact on our estimation given a short accumulation time of a few seconds.

3.5.3 Putting It All Together. As an example, Figure 10 shows the voltage traces of the capacitor when a subject is doing different activities. We can observe that, for all the five activities, our hardware ensures an approximately linear increase in the capacitor voltage when it is powered by the energy harvester. As the energy generation rates of different human activities are distinct, we can achieve activity recognition by simply using the increment rate of the capacitor voltage (i.e., the slopes of the voltage traces shown in Figure 10). Moreover, we can also notice that the capacitor voltage difference among different activities increases with the accumulation time. For instance, with T_C=1s, the voltage increment rates are similar among different activities. Since

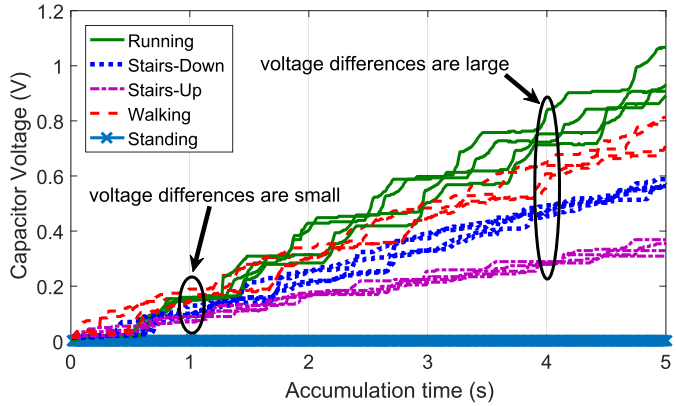

Fig. 10. An illustration of the capacitor voltage traces when the subject is doing different activities. The four traces for the same activity are plotted in the same line style. For different activities, the differences in the capacitor voltages grow with the accumulation time. Thus, it is easier to classify the activities with larger voltage sampling intervals.

CapSense merely uses the voltage increment rate for activity recognition, it will result in a high classification error. Instead, with $T_C \geq 4$s, the voltage increment among different activities is more distinctive, which results in a higher classification accuracy. In the following section, we evaluate the performance of CapSense.

4 SYSTEM EVALUATION

4.1 Experimental Setup and Data Collection

We collected our dataset from 10 healthy subjects who volunteered to do the experiments in our lab.[4] The subjects were diverse in gender (8 males and 2 females), age (range from 24 to 30), weight (from 55 to 75 Kg), and height (from 168 to 183 cm). During the data collection, the subjects were asked to wear the prototype shoe and attach the hardware board to their ankle (as shown in Figure 5(a)). We prepared shoes of different sizes to meet the requirements of our subjects.

We considered five different activities, including: walking (WALK), running (RUN), ascending stairs (SU), descending stairs (SD), and stationary (ST, i.e., sitting or standing). The subjects were asked to perform the activities normally in their own way without any specific instruction. As illustrated in Figure 11, for activities such as running and walking, they were performed in both indoor and outdoor environments to capture the influence of different terrains. For ascending and descending stairs, we conducted data collection in two building environments with different styles of stairs (i.e., the slope and steps of the stairs are different). For all the five activities, each volunteer participated in at least two data collection sessions for both indoor and outdoor environments. For walking, running, and stationary, each session lasts at least 20 seconds, while for ascending/descending stairs, each session lasts 6 to 10 seconds, depending on the number of stairs and the walking speed of the subject. For each of the five activities, we have collected at least four sessions of samples from each of the 10 subjects. In total, we have 210 sessions of data. We labeled the activity class during the data collection. The voltage of both front and rear capacitors was sampled and stored on the SD card at 100 Hz sampling rate for off-line data analysis. To compare

[4]Ethical approval for carrying out this experiment has been granted by the corresponding organization (Ethical Approval Number: HC15888).

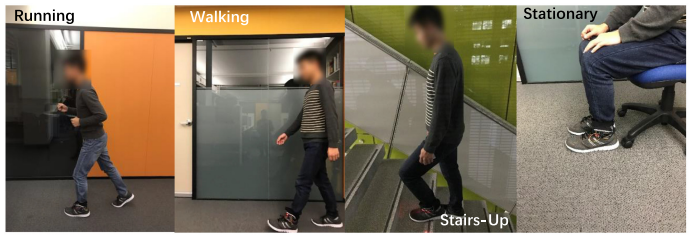

(a) Subject doing different activities.

(b) Indoor environment.

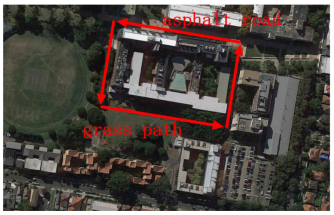

(c) Outdoor environment.

Fig. 11. The illustration of data collection.

the performance of CapSense against the transducer-based method [20], the AC voltage signal generated by the front and rear PEH was also collected simultaneously.

Recall our discussions in Section 3.5 that CapSense leverages the increasing rate r over the last accumulation time of T_C for activity recognition. Following Equation (4), we calculate the r of different activities with different T_C for all the 10 subjects using our dataset. The estimated set of r is then used as input for activity classification.

4.2 Activity Recognition Performance

The evaluation is carried out in WEKA[5] using 10-fold cross-validation with 10 repetitions for each test. Four typical machine learning algorithms are used: the C4.5 decision tree algorithm (C4.5) [43], IBk K-Nearest Neighbor classifier [1], Naive Bayes with kernel estimation [16], and RandomForest [6]. Those classifiers have been widely used in activity recognition and shown to be effective with high accuracy [7]. The parameters of the classifiers are optimized using the CVParameterSelection algorithm [21]. In the following, we evaluate the performance of CapSense given different subjects, positions of the PEH, energy accumulation times, and classifiers. In addition, we also compare its performance against the transducer-based method [20].

4.2.1 Recognition Accuracy vs. Subject. Intuitively, the foot-strike pressures applied on the energy harvesters differ in the ways that the subjects perform the activity. In the following, we consider RandomForest as the classifier and fix the accumulation window $T_C = 6s$ to investigate the impact of the subject difference on the classification accuracy.

First, we train the classifier for each of the 10 subjects in the subject-dependent manner and apply the 10-fold cross-validation for testing. Figure 12(a) exhibits the achieved accuracy for all the 10 subjects. We can notice that the accuracy varies with the subject. For example, Subject 4 achieves 75.50% of accuracy when we use the voltage samples from the Front PEH as signal, whereas Subject 6 achieves a much higher accuracy of 96.75% with the same PEH. The corresponding confusion

[5]WEKA: http://www.cs.waikato.ac.nz/ml/weka/.

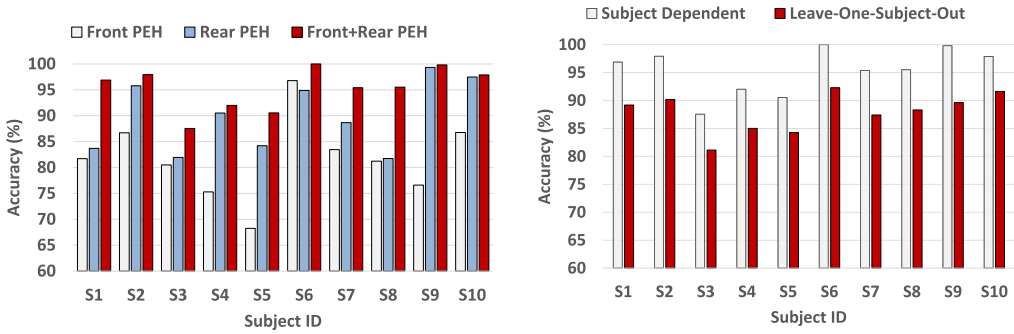

(a) CapSense performance when classifier is trained in subject-dependent manner.

(b) CapSense performance when classifier is trained in leave-one-subject-out manner.

Fig. 12. CapSense recognition accuracy (in %) achieved for all the 10 subjects. The classifier is RandomForest and the accumulation windows are fixed as $T_C = 6s$.

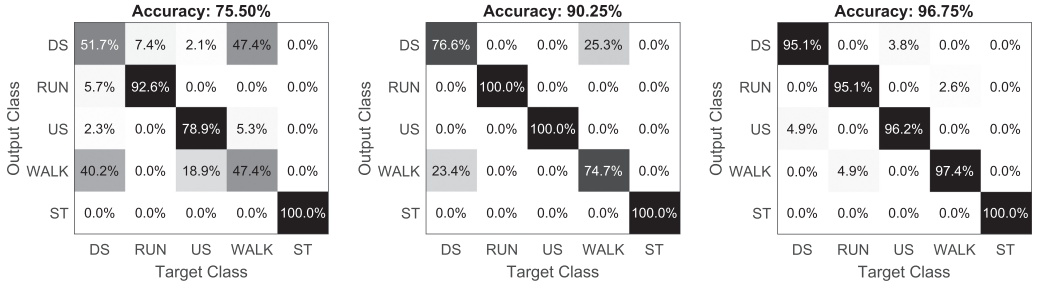

(a) Subject 4, Front PEH.

(b) Subject 4, Rear PEH.

(c) Subject 6, Front PEH.

Fig. 13. Confusion matrix of CapSense with the RandomForest classifier for Subject 4 and Subject 6. The $T_C = 6s$.

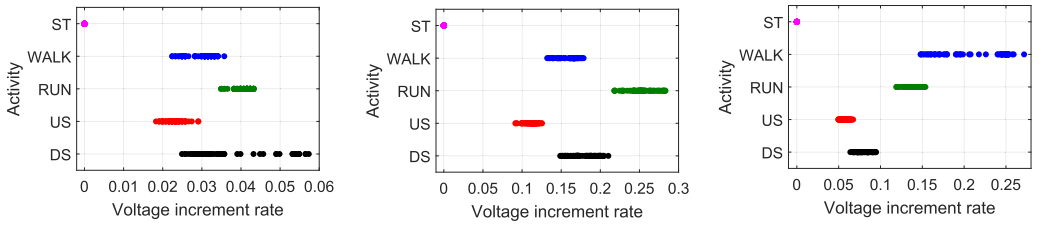

(a) Subject 4, Front PEH.

(b) Subject 4, Rear PEH.

(c) Subject 6, Front PEH.

Fig. 14. Scatter plots of the voltage increment rate of the capacitor when it is charged by the energy harvested from different activities. The Y-axis indicates the activity class, while the X-axis indicates the estimated capacitor voltage increment rate r over an accumulation time T_C of 6 s. Each dot indicates an estimated instance of r for a given activity.

matrix is given in Figure 13. In addition, the scatter plots in Figure 14 visualize all the instances of r given different activities.

As shown in Figure 13(a), the confusion matrix indicates that the major error happens in the classification between "WALK & DS" and the classification between "WALK & DS." This results from the high similarity in the voltage increment rate r when Subject 4 is performing those activities. As shown in Figure 14(a), we can observe a high overlapping in r between the "WALK,"

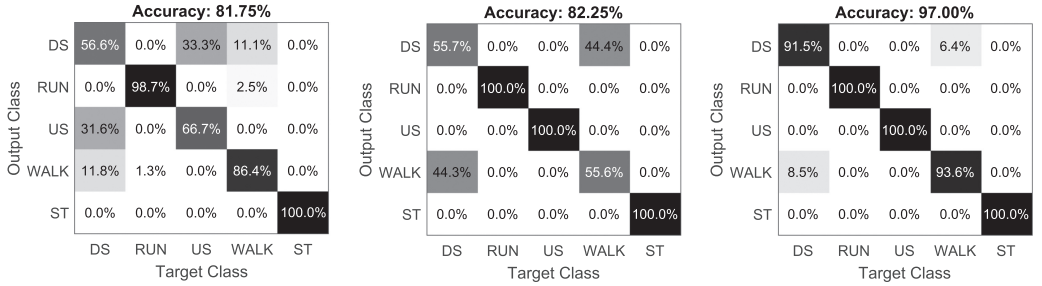

(a) Front PEH. (b) Rear PEH. (c) Front + Rear PEHs.

Fig. 15. The confusion matrices for Front, Rear, and Front+Rear PEH, respectively. The $T_C = 6s$.

"US," and "DS." That means, for Subject 4, the voltage increment rates of the capacitor are similar when it is charged by the energy harvested from those activities. This leads to a low accuracy of 75.5%. Different from Subject 4, Subject 6 performs those activities in a different way. As shown in Figure 14(c), the voltage increment rates of the capacitor are more diverse when powered by those activities. We can notice a limited number of samples are overlapped among them; this leads to a much higher classification accuracy, as shown in the confusion matrix given in Figure 13(c).

We carry out the ***leave-one-subject-out*** cross-validation over the data collected from the 10 subjects. In particular, we use data from 1 user as the testing set and the data collected from the remaining 9 subjects as the training set. This is to evaluate the robustness of CapSense against user variance and analyze the system sensitivity to subject difference. As shown in Figure 12(b), the user variance has a big impact on classification accuracy. All the 10 subjects have suffered more than 6% accuracy drop. This is because the subjects perform the same activity in different ways (i.e., subjects have different locomotion patterns) [39]. As a result, the energy that is harvested from the same activity will be different among the subjects, and it will cause variations in the voltage increment rate of a particular activity. Note that the variations result from the diversity in the subjects' locomotion patterns, rather than the difference in a particular metric (e.g., difference in weight, height, and age). The results suggest that a subject-dependent model should be considered in the practical design of our system to achieve better performance. In this regard, we conduct all the following experiments in a subject-dependent manner.

4.2.2 Recognition Accuracy vs. Different PEH. In the following, we examine the accuracy achieved by using different PEHs and investigate the performance when we fuse the signal from the two PEHs for sensing.

As shown in Figure 12(a), we can achieve a higher classification accuracy for most of the subjects (except Subject 6) by using the signal from the Rear PEH. Taking Subject 4 as an example, we can notice from Figure 14(b) that the voltage increment rate is more separated among different activities for the Rear PEH when comparing to that of the Front PEH shown in Figure 14(a). This observation matches with the confusion matrix given in Figure 13(b), in which only a small fraction of confusions happen between class "WALK" and "DS."

Moreover, CapSense achieves a better performance by fusing the signal from the two PEHs. That is to say, a two-dimensional vector, $< r_{Rear}, r_{Front} >$, is used as the input for classification, in which r_{Rear} and r_{Front} refer to the capacitor voltage increment rate of the Rear and the Front PEH, respectively. As an example, the scatter plot in Figure 16 shows the measured samples of r_{Rear} and r_{Front} when Subject 1 is doing different activities. We can notice that the r_{Front} of "DS" and "US" are similar to each other (as shown in Figure 16, if we only use r_{Front} in the Y-axis for classification, most samples of "DS" and "US" will fall in the same range from 0.1 to 0.16). That

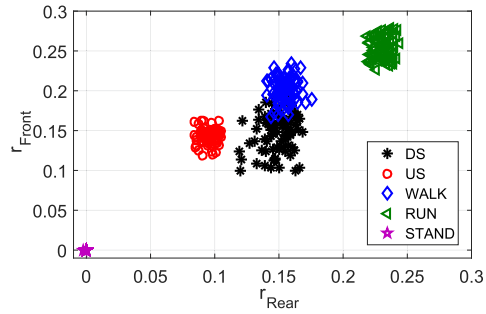

Fig. 16. The scatter plot exhibits the samples of the two-dimensional vector, $< r_{Rear}, r_{Front} >$, when Subject 1 is doing different activities. The X and the Y-axis indicate the capacitor voltage increment rate r of the Rear and the Front PEH, respectively.

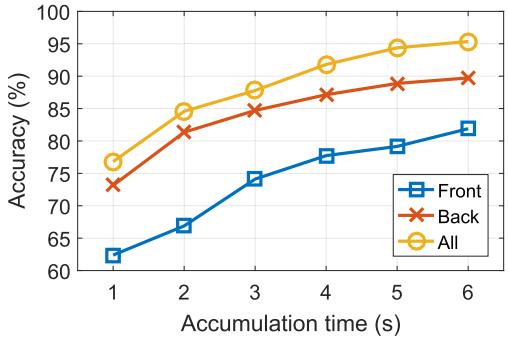

Fig. 17. The accuracy (in %) achieved by CapSense given different accumulation window T_C. The results are averaged across the 10 subjects. The classifier is RandomForest.

means, when Subject 1 performs the "DS" and "US," the Front PEH generates a similar amount of energy from those two activities. As a result, it will be hard to differentiate "DS" and "US" by using r_{Front} only. As shown in Figure 15(a), we can see a high classification error between "DS" and "US." Similar results apply to the Rear PEH as well. In Figure 16, if we only use r_{Rear} in the X-axis for classification, we can notice a high overlap between "DS" and "WALK" in r_{Rear}. Again, this results in a high classification error, as shown in Figure 15(b). However, as shown in Figure 15(c), after fusing the signal of the two PEHs, the confusions between those classes are significantly resolved. As exhibited in Figure 16 and 15(c), after applying the two-dimensional voltage vector for classification, only a small fraction of samples are misclassified between "WALK" and "DS."

4.2.3 Recognition Accuracy vs. Accumulation Time. Now, we investigate the impact of accumulation time T_C on the recognition accuracy. Figure 17 shows the achieved accuracy given different T_C. The classifier used in this experiment is the RandomForest. For a particular T_C, the reported results are the averaged accuracy across all the 10 subjects. We can clearly observe that, regardless of the signal that has been used, the accuracy increases with T_C. As shown previously in Figure 10, a larger accumulation window leads to a more distinctive difference in the capacitor voltage. Thus, a large T_C is preferable in improving the classification accuracy. However, the sojourn time in performing a specific activity is short, and transitions between activities may occur in the middle of T_C. Therefore, T_C should not be set so large that it exceeds the activity sojourn time. As reported in Reference [54], for activities such as walking, running, and standing/sitting, the sojourn time

Table 1. The Accuracy (in %) Achieved by CapSense with Different Classifiers Given Accumulation Window $T_C = 5s$

	Classifier			
	Naive Bayes	IBK	J48	RandomForest
Front PEH	78.95	78.11	79.62	78.36
Back PEH	89.46	88.63	89.11	88.88
Front+Back	95.08	93.83	94.57	94.87

The results are averaged accuracy across the 10 subjects.

Table 2. List of Features That Are Used by Transducer-based Method

Time domain features		**Frequency domain features**	**Vibration-based features**
Mean	Variance	Dominant frequencies	Mean of peaks
Standard deviation	Minimum	Dominant frequency ratio	Mean of distance between peaks
Maximum	Range	Entropy	Max distance between peaks
Absolute Mean	Coefficient variation	Energy	Max of peaks
Skewness	Interquartile range		Peak to peak difference
Kurtosis	1st, 2nd, 3rd Quartile		
Absolute Area	Mean crossing rate		
Mean of absolute value	Root mean square		

is at least 1 to 2 minutes. For activities such as ascending/descending stairs, the sojourn time is much shorter, but still longer than 5 seconds for over 99.9% of the time. During our data collection, we have noticed that, for ascending/descending a 10-step set of stairs, the sojourn time is usually within 6 to 10 seconds, depending on the subject's speed. Therefore, as a trade-off between the system performance and robustness, we recommend the maximum value of T_C for CapSense to be configured to 5 seconds. As shown in Figure 17, after fusing the signal from Front and Back PEHs, CapSense is able to achieve 95% of accuracy with $T_C = 5s$.

4.2.4 Recognition Accuracy v.s. Classifier. Table 1 presents the accuracy of CapSense with different classifiers given $T_C = 5s$. The results are averaged across all the 10 subjects. We can observe that all the four examined classifiers can achieve over 93% of accuracy after fusing the signal from the two PEHs. This performance is comparable to that achieved by conventional motion-sensor-based systems [30]. An interesting observation is that CapSense exhibits no bias on the selection of classifier, as all the four classifiers achieved similar classification results.

4.2.5 Compare against Transducer-based Method. In the following, we compare the performance of CapSense against the conventional transducer-based method [20]. For both CapSense and tranducer-based, the signals from the two PEHs are fused to improve accuracy. In case of transducer-based method, we consider different window sizes with a variety of sampling frequencies. We extract 25 features from the AC voltage signal as the input for classification. The details of the features are shown in Table 2. The classifier used in this experiment is the Naive Bayes.

Table 3 shows the achieved accuracy for all the methods given different window sizes. The results are averaged across all the 10 subjects. In addition, Table 4 gives the total MCU wake-up times needed by different methods to achieve the same recognition accuracy. As shown in Table 4, by using all the 25 features, transducer-based method still needs to sample the signal at 25 Hz to achieve a comparable accuracy with CapSense. In the case that only the mean feature is used, transducer-based method needs to sample at least 50 Hz to achieve the same accuracy. This implies

Table 3. The Accuracy (in %) Achieved by CapSense Compared against That of the Transducer-based Method

Window Size	CapSense	Transducer-based									
		Set of 25 Features					Mean Feature Only				
		100Hz	50Hz	25Hz	10Hz	5Hz	100Hz	50Hz	25Hz	10Hz	5Hz
6S	95.1	98.2	97.8	96.6	94.7	92.2	96.4	95.7	94.2	88.9	84.3
5S	94.6	97.3	96.8	95.6	91.1	86.9	95.8	94.7	92.3	82.4	78.0
4S	93.1	96.9	95.3	93.1	86.4	81.3	94.4	93.2	89.2	70.7	66.2
3S	87.3	93.2	92.4	91.6	83.6	80.3	89.3	87.2	78.9	68.3	64.7
2S	83.4	91.6	88.6	83.6	77.1	68.3	84.2	83.3	75.6	65.8	60.5
1S	75.7	76.2	75.6	72.2	70.2	64.2	76.1	75.5	70.2	64.2	58.4

The results are averaged across the 10 subjects.

Table 4. The Total MCU Wake-up Times Needed by Different Methods to Achieve the Same Recognition Accuracy

Window Size	Accuracy Target	Total MCU Wake-up Time		
		CapSense	Transducer-based (25 features)	Transducer-based (mean feature)
6 s	95%	1	25 Hz × 6 = 150	50 Hz × 6 = 300
5 s	94%	1	25 Hz × 5 = 125	50 Hz × 5 = 250
4 s	93%	1	25 Hz × 4 = 100	50 Hz × 4 = 200
3 s	87%	1	25 Hz × 3 = 75	50 Hz × 3 = 150
2 s	83%	1	25 Hz × 2 = 50	50 Hz × 2 = 100
1 s	75%	1	50 Hz × 1 =50	50 Hz × 1 =50

that CapSense can significantly reduce the required sampling frequency and the total MCU wake-up time without sacrificing the recognition accuracy.

5 ENERGY CONSUMPTION ANALYSIS

High energy consumption is the major roadblock for the pervasive use of wearable technology [46]. In this section, we will conduct an extensive power-consumption profiling of the off-the-shelf wearable activity recognition systems to investigate the superiority of CapSense in energy saving.

5.1 Setup for Energy Consumption Analysis

We use an off-the-shelf Texas Instruments SensorTag[6] as the target device, which is embedded with the ultra-low power ARM Cortex-M3 MCU that is specifically designed for today's energy-efficient wearable devices.[7] The SensorTag is running the Contiki 3.0 operating system,[8] which duty-cycles the MCU to save energy. Moreover, all unnecessary components, including the onboard ADC, SPI bus, and the onboard accelerometers are powered off when it is not sampling. We are interested in the power consumption of SensorTag in data sampling (i.e., either in sampling the capacitor voltage

[6]SensorTag: http://www.ti.com/ww/en/wireless_connectivity/sensortag/.
[7]Mainstream wearable devices such as FitBit are using ARM Cortex-M3: see https://www.ifixit.com/Teardown/Fitbit+Flex+Teardown/16050.
[8]Contiki OS: http://www.contiki-os.org/.

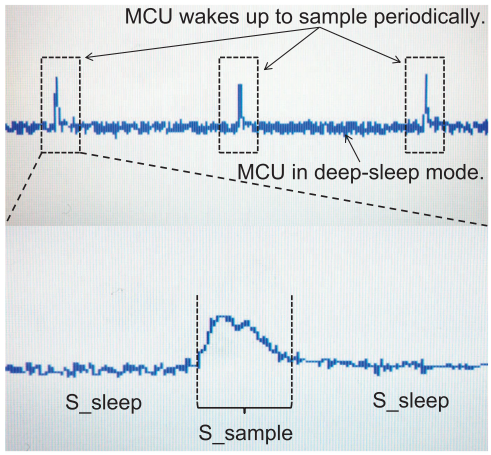

Fig. 18. Profiling of voltage sampling.

Table 5. States of MCU in Sampling the ADC Signal

State	**Time** (ms)	**Power** (μW)	**Description**
S_{sample}	0.6	480	MCU wakes up to sample ADC signal.
S_{sleep}	null	6	MCU in deep-sleep mode.

or the AC voltage signal from KEH-transducer) and the power consumption in data transmission. The average power consumption and time requirement for each sampling and transmission event are measured by using the built-in function in the Agilent DSO3202A oscilloscope. In the following, we present our measurement results of those parts in order.

5.2 Power Consumption in Sampling

First, we investigate the power consumption in data sampling. In the measurement, both capacitor voltage and KEH-transducer signal are sampled through the onboard ADC of SensorTag. Figure 18 presents an oscilloscope trace when MCU sampling the signal from ADC periodically. As shown, MCU is triggered by the timer to sample periodically. It takes approximately 0.6 *ms* for the MCU to complete a single voltage sampling event (i.e., state S_{sample} shown in Figure 18). After that, MCU turns back into the deep sleep mode (i.e., LPM3 in Contiki OS) to save power. The average power consumption of the system for a single ADC sampling is 480 μW, and the baseline system power consumption when MCU is in the deep-sleep mode is only 6 μW. The details are summarized in Table 5.

In general, for the duty-cycled activity sensing system, the average power consumption in data sampling, P_{sense}, can be obtained by the following equation:

$$P_{sense} = \begin{cases} \frac{T_S \times n}{1000} P_{sample} + P_{sleep} - \frac{T_S \times n}{1000} \times P_{sleep} & \text{if } 0 \leq n \leq \frac{1000}{T_S}, \\ P_{sample} & \text{if } \frac{1000}{T_S} < n, \end{cases} \tag{5}$$

where, P_{sample} is the average power consumption of the system during the sampling event, and P_{sleep} is the average power consumption when the MCU is in deep-sleep mode (with all the other system components powered off). n is the sampling frequency, and T_S is the duration of time (in milliseconds) required by a single sampling event. Based on the measurement results given in

Table 6. The Power Consumption (μW) in Data Sampling

	KEH-transducer (Mean feature)	KEH-transducer (25 features)	CapSense-0.2 Hz
Sensing	14.22	7.11	0.06
MCU Sleep	6	6	6
Overall	20.22	13.11	6.06

Table 5, we can have the average power consumption for KEH voltage sampling event, P_{sample}, equal to 480 μW with a duration, T_S, equal to 0.6 ms. The power consumption when MCU is in deep-sleep mode, P_{sleep}, is 6 μW.

As discussed in Table 4, for KEH-transducer-based system, given different feature sets, a sampling frequency of 2 5 Hz–50 Hz is required to achieve recognition accuracy as good as CapSense. For transducer-based with 25 features, the minimum required sampling frequency is 25 Hz. Therefore, following Equation (5), we can obtain the power consumption in data sampling for KEH transducer-based system is 13.11 μW. Similarly, for transducer-based with mean feature only, the power consumption in data sampling increases to 20.22 μW. However, as demonstrated in Section 4, to achieve an overall classification accuracy of 94%, CapSense only needs to sample the ADC signal once every 5 s. Thus, given Equation (5), the power consumption in data sampling for CapSense is only 6.06 μW.

The results are compared in Table 6. As shown, **CapSense is able to save 70% and 54% of the overall power consumed by the transducer-based system in data sampling given different features being used**. We can also notice that, for CapSense, the main energy expenditure is the MCU Sleep (i.e., the unavoidable power consumption of the system when MCU is in the deep-sleep mode), which consumes 99% (6 μW over 6.06 μW) of the overall sampling power consumption. Fortunately, with the rapid development of energy-efficient micro-controllers, we can expect the power consumption of MCU Sleep to be further reduced. For instance, the STM32L4 Series of MCUs[9] consume only 1.35 μW in its sleep mode; it can help CapSense achieve an ultra-low system power consumption of 1.41 μW.

5.3 Power Consumption for Data Transmission

In the following, we investigate the power consumption in wireless data transmission using the BLE beacons. We programmed the Contiki OS to wake up the CC2650 wireless MCU periodically and transmit a BLE beacon packet, which broadcasts three times on three separate channels (repetition improves reliability of broadcasting). The transmitted beacon packets are all 19 Bytes (all for protocol payloads. The details for each BLE broadcasting event are visualized in Figure 19 and summarized in Table 7. Note that the transmission time is depending on the packet size. The time stated in Table 7 (0.28 ms for state S2, S4, and S6) is the minimum required time to transmit the 19 Bytes packet per channel. For every additional Byte[10] to be transmitted, 8 μs time needs to be added to the total transmission time.

For CapSense, it has only two samples to be transmitted once every five seconds (in total, 4 Bytes) for the voltages of the front and rear capacitors. This results in one packet to be transmitted per channel. The total energy consumption in transmission for CapSense is 7.61 μJ.[11] The

[9]STM32L4 Series: http://http://www.st.com/en/microcontrollers/stm32l4-series.html.
[10]According to the protocol, up to 28 Bytes of data could be added to the 19 Bytes payloads per packet.
[11]Obtained by: $1.12\ ms \times 1.008\ mW + 1.72\ ms \times 0.744\ mW + 3 \times 0.312\ ms \times 3.99\ mW + 2 \times 0.3\ ms \times 2.46\ mW = 7.61\ \mu J$.

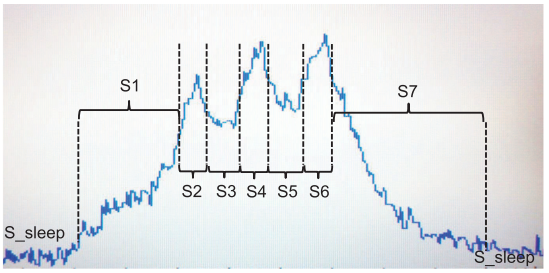

Fig. 19. Profiling of BLE broadcasting event.

Table 7. States of BLE Broadcasting Event

State	**Time** (ms)	**Power** (uW)	**Description**
S1	1.12	1,008	Radio setup.
S2, S4, S6	0.28	3,990	Radio transmits a beacon packet of 19 Bytes.
S3, S5	0.30	2,460	Transition between transmissions.
S7	1.72	744	Post-processing before sleep.
S_sleep	null	6	Radio off; MCU in deep-sleep mode.

Table 8. Summary of Data Transmission Power Consumption

	Transducer (mean feature)	**CapSense-0.2 Hz**
Transmission Energy	7.61 μJ	7.61 μJ
Feature Extraction Energy	16.25 μJ	0
Total Energy	23.86 μJ	7.61 μJ

average power consumption is 1.747 mW with time duration of 4.3 ms; similarly for transducer-based methods, if considering the case where the features are extracted onboard and only the selected features will be transmitted. In the best scenairo, transducer-based method needs to transmit only two samples for the mean features of front and rear PEH, respectively. This results in same transmission power as CapSense. However, to extract the two mean features, it consumes 16.25 μJ of energy [11]. The results are compared in Table 8. As shown, CapSense is able to **save over 68.1% of the energy consumption in data transmission**. Clearly, for KEH-transducer-based systems, the additional onboard computations for feature selection have introduced inevitable power consumption.

Combining the power consumption in data sampling and transmission together, the overall system power consumption for KEH-transducer-based system is 17.79 μW,[12] whereas the overall system power consumption for CapSense is only 7.58 μW.[13] This means that **CapSense is able to save 57% of the overall system power consumption of state-of-the-art KEH-transducer-based system**.

6 RELATED WORK

In this section, we first review the efforts in building insole-based self-powered wearable system. Then, we introduce some recent efforts in using KEH-transducer as the motion sensor for

[12]Obtained by:$(\frac{13.11\mu W\times 5sec+23.86\mu J}{5sec+4.3ms}) = 17.79\ \mu W$.

[13]Obtained by:$(\frac{6.06\mu W\times 5sec+7.61\mu J}{5sec+4.3ms}) = 7.58\ \mu$W.

energy-efficient sensing. Last, we review some works in reducing sampling-induced power consumption by finding the minimum required sampling frequency for conventional motion-sensor-based activity recognition systems.

6.1 Insole-based Energy Harvesting System

With recent advances in energy harvesting hardware, researchers are now turning to kinetic energy harvesting as a viable source of power to extend battery life or even replace the batteries altogether in wearable devices [37, 40]. Some wearable KEH products are already appearing in the market, such as AMPY wearable motion charger [2], SEQUENT self-charing smartwatch [47], and SOLEPOWER energy harvesting shoe [49], showing signs of a promising future for this technology. In the context of wearable shoes, insole-based kinetic energy harvesting is widely regarded as the most popular solution to achieve self-power given the high harvesting efficiency from human walking [3]. The history of building shoe-based self-powered wearable devices started in the late '90s. In an earlier work of Antaki et al. [3], the authors discovered that the ground reaction forces associated with the heel strike and toe-off phases of the gait can generate the largest amount of energy during human walking. In this study, a piezoelectric array-based EH shoe has been built to generate electric energy from human gait. Similarly, in the work of Kymissis et al. [24], a piezoelectric generator is placed inside the shoe and can generate 1.1–1.8 mW average power during walking. They have proved that the generated energy is able to power the RFID transmitter to broadcast signal periodically. More recently, in Reference [36], a shoe-mounted energy harvesting system has been developed for podiatric analysis. A piezoelectric energy harvester was leveraged to generate 10–20 μJ energy per walking step. A pressure sensor and passive foot-strike sensor were utilized to analyze human gaits. Another example of self-powered shoe is given by Huang et al. [14]. Their prototype consists of a pair of shoes, an accelerometer, and Bluetooth wireless communication unit powered separately by the energy harvested from each of the two feet, and coordinated by ambient backscatter. The accelerometer can sense the activity of the user, while the Bluetooth can transmit the sensing results to the smartphone. Different from the aforementioned efforts that focus either on maximizing the amount of harvesting energy or optimizing the wearable system to achieve self-power, the focus and contribution of our work is to investigate the feasibility of utilizing the capacitor voltage to achieve daily activity recognition while dramatically reducing the required sampling frequency. To the best of our knowledge, this has not been studied in the current literature yet.

6.2 Energy Harvesting–based Context Sensing

6.2.1 Energy Transducer-based Sensing. In the current literature, tremendous efforts have been made in leveraging energy transducers, as sensors to derive different contextual information. For instance, in Reference [20], Khalifa et al. proposed the idea of using the power signal generated by a KEH device for human activities recognition. The proposed system can achieve 83% of accuracy for classifying different daily activities. Similarly, in Reference [17], a piezoelectric transducer-based wearable necklace has been designed for food-intake monitoring. The proposed system achieves over 80% of accuracy in distinguishing food categories. Li et al. [32] designed an energy harvesting device powered by the airflow from an air-conditioning system. The instantaneous energy output were used to monitor the usage of the air-conditioning system. In Reference [28], the authors investigate the feasibility of using KEH as the sensor for transportation mode detection. In Reference [5], Blank et al. proposed a ball impact localization system using a piezoelectric embedded table tennis racket. More recently, Xu et al. [53] and Ma et al. [34] have studied the use of kinetic energy signal for mobile user authentication system based on gait analysis. In References [26, 29], the authors proposed the use of KEH-transducer as an energy-efficient receiver for acoustic communication.

Although transducer-based systems can save the energy in powering the motion sensor, they cannot prevent the MCU from waking up to read every new energy signal. In contrast, the state-of-the-art MEMS sensors are embedded with the First-In First-Out (FIFO) buffer to store the acceleration signal and save the MCU from reading every sample. It has been reported that transducer-based systems can save up to 79% of the overall system power consumption of the accelerometer-based systems [20]. However, this is estimated under the assumption that no FIFO buffer has been used. Different from existing works, in this article, we try to leverage the natural characteristic of capacitor to overcome the current disadvantage of transducer-based systems (i.e., no FIFO buffer to store the samples). In our design, the capacitor performs like the FIFO to accumulate energy readings and prevents MCU from waking up.

6.2.2 Capacitor-based Sensing. Unlike most MEMS sensors that are embedded with the FIFO buffer to store samples, energy transducers cannot prevent the MCU from waking up to read every new energy signal. Thus, as discussed, a considerable amount of limited harvested power will be consumed by the MCU. In addition to using energy transducer as sensor, the accumulated energy information provided by the energy storage, i.e., capacitor or rechargeable battery, can also be used for sensing. For instance, in Reference [44], by analyzing the "stairs" in the voltage waveform of the the capacitor, the proposed system can estimate the number of steps the user has walked. Intuitively, this is simply because the pressure from the human foot will blend the energy harvester to charge the capacitor during walking. Similarly, in Reference [18], the authors proposed a foot-mounted energy harvesting system. The energy harvested from walking was stored in a capacitor. Once the capacitor voltage exceeds a pre-defined threshold, it will be discharged to power a BLE beacon transmission. When the capacitor voltage decreases below the voltage threshold, the BLE transmission will stop until the capacitor voltage reaches the threshold again. Based on the beacon transmission rate, a step counts estimation algorithm is designed. In addition to human-centric sensing, the authors in Reference [10] developed an electromagnetic energy harvester–based power meter to estimate the current load in power lines. The underlying intuition is that the energy harvesting rate of the electromagnetic energy harvester is proportional to the strength of the induced magnetic field—namely, the strength of current flow in the power lines. Once the voltage of the capacitor exceeds a predefined threshold, a pulse transmission will be triggered. Using the signal receiving rate, the energy harvesting rate and current load can be estimated. Different from the existing efforts that rely on radio transmitter [10, 18] or focus only on simple pedometer application [44], CapSense can classify five different daily activities by merely reading the capacitor voltage once every five seconds.

6.3 Reducing Sampling Frequency

For both KEH-transducer-based and conventional motion-sensor-based systems, the energy consumption in sensing is proportional to the sampling frequency. Thus, a large volume of works in the literature focused on reducing the sampling rates to save the energy [7, 11, 42, 54] to improve the system energy efficiency. For instance, in Reference [23], Krause et al. studied the trade-off between the system power consumption and classification accuracy by using a smartwatch wearable device. They demonstrated that the lifetime of the device can be extended by selecting the optimal sampling strategy without losing accuracy. Similar results are presented in Reference [54], in which the authors pointed out that there is a trade-off between sampling frequency and classification accuracy; and they introduced the A3R algorithm, which adapts the sampling frequency and classification features in real-time based on the activity type. In addition, by leveraging the temporal-sparsity of human activity, researchers have also proposed the use of compressive sensing theory to reduce sampling frequency [8, 33, 41]. Instead of reducing the sampling frequency

to the level of tens of Hz, in this work, we introduce CapSense to bring the sampling frequency down to 0.2 Hz.

7 CONCLUSION

In this article, we present CapSense, a novel activity-sensing scheme for KEH-powered wearable devices. By sampling the voltage readings of the energy harvesting capacitor at 0.2 Hz, CapSense is able to classify five different daily activities with 95% accuracy while reducing system power consumption by 57%. However, in spite of the promise, CapSense is still in its infancy. Further efforts are needed to fully realize its potential. First, as the current prototype is cumbersome, one possible direction for future work is to design the hardware with a smaller form-factor. Detailed study on the practical user experience of the device is also needed. Second, as the hardware can harvest energy from the human activity, we will investigate comprehensive system design to power the system using the harvested energy and make it battery-free. Last, in addition to human activity recognition, we would like to explore the feasibility of CapSense in other application scenarios. For instance, instead of using kinetic energy harvester, we can use the thermo and solar energy harvesters to charge the capacitor. By using the capacitor voltage, it may introduce new opportunities in monitoring the usage of hot water and indoor lights.

REFERENCES

[1] David W. Aha, Dennis Kibler, and Marc K. Albert. 1991. Instance-based learning algorithms. *Mach. Learn.* 6, 1 (1991), 37–66.

[2] AMPY. 2016. Ampy Move Wearable Motion Charger. Retrieved from http://www.getampy.com/.

[3] James F. Antaki, Gina E. Bertocci, Elizabeth C. Green, Ahmed Nadeem, Thomas Rintoul, Robert L. Kormos, and Bartley P. Griffith. 1995. A gait-powered autologous battery charging system for artificial organs. *ASAIO J.* 41, 3 (1995), M588–95.

[4] Naveed Anwar Bhatti, Muhammad Hamad Alizai, Affan A. Syed, and Luca Mottola. 2016. Energy harvesting and wireless transfer in sensor network applications: Concepts and experiences. *ACM Trans. Sens. Netw.* 12, 3 (2016), 24.

[5] Peter Blank, Thomas Kautz, and Bjoern M. Eskofier. 2016. Ball impact localization on table tennis rackets using piezoelectric sensors. In *Proceedings of the ACM International Symposium on Wearable Computers*. 72–79.

[6] Leo Breiman. 2001. Random forests. *Mach. Learn.* 45, 1 (2001), 5–32.

[7] Andreas Bulling, Ulf Blanke, and Bernt Schiele. 2014. A tutorial on human activity recognition using body-worn inertial sensors. *Comput. Surv.* 46, 3 (2014), 33.

[8] Chun Tung Chou, Rajib Rana, and Wen Hu. 2009. Energy efficient information collection in wireless sensor networks using adaptive compressive sensing. In *Proceedings of the IEEE Conference on Local Computer Networks*. 443–450.

[9] Sunny Consolvo, David W. McDonald, Tammy Toscos, Mike Y. Chen, Jon Froehlich, Beverly Harrison, Predrag Klasnja, Anthony LaMarca, Louis LeGrand, Ryan Libby, et al. 2008. Activity sensing in the wild: A field trial of UbiFit garden. In *Proceedings of the SIGCHI Conference on Human Factors in Computing Systems*. ACM, 1797–1806.

[10] Samuel DeBruin, Bradford Campbell, and Prabal Dutta. 2013. Monjolo: An energy-harvesting energy meter architecture. In *Proceedings of the ACM Conference on Embedded Networked Sensor Systems*. 18:1–18:14.

[11] Hassan Ghasemzadeh, Navid Amini, Ramyar Saeedi, and Majid Sarrafzadeh. 2015. Power-aware computing in wearable sensor networks: An optimal feature selection. *IEEE Trans. Mob. Comput.* 14, 4 (2015), 800–812.

[12] Maria Gorlatova, John Sarik, Guy Grebla, Mina Cong, Ioannis Kymissis, and Gil Zussman. 2015. Movers and shakers: Kinetic energy harvesting for the internet of things. *IEEE J. Select. Areas Commun.* 33, 8 (2015), 1624–1639.

[13] Mahbub Hassan, Wen Hu, Guohao Lan, Sara Khalifa, Aruna Seneviratne, and Sajal K. Das. 2018. Kinetic-powered wearable IoT for healthcare: Challenges and opportunities. *IEEE Comput.* 51, 9 (2018), 64–74.

[14] Qianyi Huang, Yan Mei, Wei Wang, and Qian Zhang. 2015. Battery-free sensing platform for wearable devices: The synergy between two feet. In *Proceedings of the IEEE International Conference on Computer Communications*. 1–9.

[15] Koichi Ishida, Tsung-Ching Huang, Kentaro Honda, Yasuhiro Shinozuka, Hiroshi Fuketa, Tomoyuki Yokota, Ute Zschieschang, Hagen Klauk, Gregory Tortissier, Tsuyoshi Sekitani, et al. 2013. Insole pedometer with piezoelectric energy harvester and 2V organic circuits. *IEEE J. Solid-State Circ.* 48, 1 (2013), 255–264.

[16] George H. John and Pat Langley. 1995. Estimating continuous distributions in Bayesian classifiers. In *Proceedings of the Conference on Uncertainty in Artificial Intelligence*. Morgan Kaufmann Publishers Inc., 338–345.

[17] Haik Kalantarian, Nabil Alshurafa, Tuan Le, and Majid Sarrafzadeh. 2015. Monitoring eating habits using a piezoelectric sensor-based necklace. *Comput. Biol. Med.* 58 (2015), 46–55.

[18] Haik Kalantarian and Majid Sarrafzadeh. 2016. Pedometers without batteries: An energy harvesting shoe. *IEEE Sens. J.* 16, 23 (2016).
[19] Matthew Keally, Gang Zhou, Guoliang Xing, Jianxin Wu, and Andrew Pyles. 2011. PBN: Towards practical activity recognition using smartphone-based body sensor networks. In *Proceedings of the ACM Conference on Embedded Networked Sensor Systems*. ACM, 246–259.
[20] Sara Khalifa, Guohao Lan, Mahbub Hassan, Aruna Seneviratne, and Sajal K. Das. 2018. HARKE: Human activity recognition from kinetic energy harvesting data in wearable devices. *IEEE Trans. Mob. Comput.* 17, 6 (2018), 1353–1368.
[21] R. Kohavi. 1995. *Wrappers for Performance Enhancement and Oblivious Decision Graphs*. Ph.D. Dissertation. Stanford University, Department of Computer Science, Stanford University.
[22] Kyoungchul Kong and Masayoshi Tomizuka. 2008. Smooth and continuous human gait phase detection based on foot pressure patterns. In *Proceedings of the IEEE International Conference on Robotics and Automation*. 3678–3683.
[23] Andreas Krause, Matthias Ihmig, Edward Rankin, Derek Leong, Smriti Gupta, Daniel Siewiorek, Asim Smailagic, Michael Deisher, and Uttam Sengupta. 2005. Trading off prediction accuracy and power consumption for context-aware wearable computing. In *Proceedings of the IEEE International Symposium on Wearable Computers*. 20–26.
[24] John Kymissis, Clyde Kendall, Joseph Paradiso, and Neil Gershenfeld. 1998. Parasitic power harvesting in shoes. In *Proceedings of the IEEE International Symposium on Wearable Computers*. 132–139.
[25] Guohao Lan, Sara Khalifa, Mahbub Hassan, and Wen Hu. 2015. Estimating calorie expenditure from output voltage of piezoelectric energy harvester: An experimental feasibility study. In *Proceedings of the 10th EAI International Conference on Body Area Networks*. 179–185.
[26] Guohao Lan, Dong Ma, Mahbub Hassan, and Wen Hu. 2018. HiddenCode: Hidden acoustic signal capture with vibration energy harvesting. In *Proceedings of the IEEE International Conference on Pervasive Computing and Communications*. 1–10.
[27] Guohao Lan, Dong Ma, Weitao Xu, Mahbub Hassan, and Wen Hu. 2017. CapSense: Capacitor-based activity sensing for kinetic energy harvesting powered wearable devices. In *Proceedings of the EAI International Conference on Mobile and Ubiquitous Systems: Computing, Networking, and Services*. 106–115.
[28] Guohao Lan, Weitao Xu, Sara Khalifa, Mahbub Hassan, and Wen Hu. 2016. Transportation mode detection using kinetic energy harvesting wearables. In *Proceedings of the IEEE International Conference on Pervasive Computing and Communication*. 1–4.
[29] Guohao Lan, Weitao Xu, Sara Khalifa, Mahbub Hassan, and Wen Hu. 2017. VEH-COM: Demodulating vibration energy harvesting for short range communication. In *Proceedings of the IEEE International Conference on Pervasive Computing and Communications*. 170–179.
[30] O. D. Lara and M. A. Labrador. 2013. A survey on human activity recognition using wearable sensors. *IEEE Commun. Surv. Tutor.* 15, 3 (2013), 1192–1209.
[31] Oscar D. Lara and Miguel A. Labrador. 2013. A survey on human activity recognition using wearable sensors. *IEEE Commun. Surv. Tutor.* 15, 3 (2013), 1192–1209.
[32] Feng Li, Yanbing Yang, Zicheng Chi, Liya Zhao, Yaowen Yang, and Jun Luo. 2018. Trinity: Enabling self-sustaining WSNs indoors with energy-free sensing and networking. *ACM Trans. Embed. Comput. Syst.* 17, 2 (2018), 57.
[33] Shancang Li, Li Da Xu, and Xinheng Wang. 2013. Compressed sensing signal and data acquisition in wireless sensor networks and internet of things. *IEEE Trans. Industr. Inf.* 9, 4 (2013), 2177–2186.
[34] Dong Ma, Guohao Lan, Weitao Xu, Mahbub Hassan, and Wen Hu. 2018. SEHS: Simultaneous energy harvesting and sensing using piezoelectric energy harvester. In *Proceedings of the IEEE/ACM International Conference on Internet-of-Things Design and Implementation*. 201–212.
[35] J. Ross Macdonald and Malcolm K. Brachman. 1955. The charging and discharging of nonlinear capacitors. *Proc. Inst. Radio Eng.* 43, 1 (1955), 71–78.
[36] Rich Meier, Nicholas Kelly, Omri Almog, and Patrick Chiang. 2014. A piezoelectric energy-harvesting shoe system for podiatric sensing. In *Proceedings of the IEEE International Conference of the Engineering in Medicine and Biology Society*. 622–625.
[37] Paul D. Mitcheson, Eric M. Yeatman, G. Kondala Rao, Andrew S. Holmes, and Tim C. Green. 2008. Energy harvesting from human and machine motion for wireless electronic devices. *Proc. IEEE* 96, 9 (2008), 1457–1486.
[38] Muhammad Mubashir, Ling Shao, and Luke Seed. 2013. A survey on fall detection: Principles and approaches. *Neurocomputing* 100 (2013), 144–152.
[39] Wei Pan and Lorenzo Torresani. 2009. Unsupervised hierarchical modeling of locomotion styles. In *Proceedings of the ACM International Conference on Machine Learning*. 785–792.
[40] Joseph A. Paradiso and Thad Starner. 2005. Energy scavenging for mobile and wireless electronics. *IEEE Perv. Comput.* 4, 1 (2005), 18–27.

[41] Liu Qi, James Williamson, Wyatt Mohrman, Kun Li, Qin Lv, Robert Dick, and Li Shang. 2017. Gazelle: Energy-efficient wearable analysis for running. *IEEE Trans. Mob. Comput.* 16, 9 (2017), 2531–2544.
[42] Xin Qi, Matthew Keally, Gang Zhou, Yantao Li, and Zhen Ren. 2013. AdaSense: Adapting sampling rates for activity recognition in body sensor networks. In *Proceedings of the IEEE Real-Time and Embedded Technology and Applications Symposium*. 163–172.
[43] J. Ross Quinlan. 2014. *C4. 5: Programs for Machine Learning*. Elsevier.
[44] Alberto Rodriguez, Domenico Balsamo, Zhenhua Luo, Steve P. Beeby, Geoff V. Merrett, and Alex S. Weddel. 2017. Intermittently powered energy harvesting step counter for fitness tracking. In *Proceedings of the IEEE Conference on Sensors Applications Symposium*. 1–6.
[45] Seiko. 2016. Seiko Kinetic Watch. Retrieved from https://www.seikowatches.com/world/technology/kinetic/.
[46] Suranga Seneviratne, Yining Hu, Tham Nguyen, Guohao Lan, Sara Khalifa, Kanchana Thilakarathna, Mahbub Hassan, and Aruna Seneviratne. 2017. A survey of wearable devices and challenges. *IEEE Commun. Surv. Tutor.* 19, 4 (2017), 2573–2620.
[47] Sequent. 2018. SEQUENT Self-charging Smartwatch. Retrieved from http://www.sequentwatch.com/.
[48] Nathan S. Shenck and Joseph A. Paradiso. 2001. Energy scavenging with shoe-mounted piezoelectrics. *IEEE Micro* 21, 3 (2001), 30–42.
[49] Solepower. 2016. Solepower Energy Harvesting Shoe. Retrieved from http://www.solepowertech.com/.
[50] Svante Westerlund and Lars Ekstam. 1994. Capacitor theory. *IEEE Trans. Dielect. Elect. Insul.* 1, 5 (1994), 826–839.
[51] Longhan Xie and Mingjing Cai. 2014. Human motion: Sustainable power for wearable electronics. *IEEE Perv. Comput.* 13, 4 (2014), 42–49.
[52] Weitao Xu, Guohao Lan, Qi Lin, Sara Khalifa, Neil Bergmann, Mahbub Hassan, and Wen Hu. 2019. KEH-Gait: Using kinetic energy harvesting for gait-based user authentication systems. *IEEE Trans. Mob. Comput.* 18, 1 (2019), 139–152.
[53] Weitao Xu, Guohao Lan, Qi Lin, Sara Khalifa, Neil Bergmann, Mahbub Hassan, and Hu Wen. 2017. KEH-Gait: Towards a Mobile healthcare user authentication system by kinetic energy harvesting. In *Proceedings of the Network and Distributed Systems Security Symposium*.
[54] Zhixian Yan, Vigneshwaran Subbaraju, Dipanjan Chakraborty, Archan Misra, and Karl Aberer. 2012. Energy-efficient continuous activity recognition on mobile phones: An activity-adaptive approach. In *Proceedings of the IEEE International Symposium on Wearable Computers*. 17–24.
[55] Boram Yang and Kwang-Seok Yun. 2012. Piezoelectric shell structures as wearable energy harvesters for effective power generation at low-frequency movement. *Sens. Actuat. A: Phys.* 188 (2012), 427–433.
[56] Jaeseok Yun, Shwetak Patel, Matt Reynolds, and Gregory Abowd. 2008. A quantitative investigation of inertial power harvesting for human-powered devices. In *Proceedings of the ACM International Conference on Ubiquitous Computing*. ACM, 74–83.

Received June 2018; revised March 2019; accepted July 2019